

Proximal cysteine residues in proteins promote N^{ϵ} -carboxyalkylation of lysine residues by α -dicarbonyl compounds

Received for publication, August 29, 2024, and in revised form, February 12, 2025. Published, Papers in Press, March 4, 2025.

<https://doi.org/10.1016/j.jbc.2025.108377>

Sudipta Panja^{1,*}, Johanna Rankenberg¹, Cole Michel², Grace Cooksley¹ , Marcus A. Glomb³, and Ram H. Nagaraj^{1,2,*} 

From the ¹Department of Ophthalmology, School of Medicine, University of Colorado, Aurora, Colorado, USA; ²Department of Pharmaceutical Sciences, Skaggs School of Pharmacy and Pharmaceutical Sciences, University of Colorado, Aurora, Colorado, USA; ³Institute of Chemistry, Food Chemistry, Martin-Luther-University Halle-Wittenberg, Halle(Saale), Germany

Reviewed by members of the JBC Editorial Board. Edited by Ursula Jakob

Advanced glycation end products (AGEs) are protein modifications resulting from the chemical reaction between lysine and arginine residues in proteins, and carbonyl compounds, including glyoxal (GO) and methylglyoxal (MGO). N^{ϵ} -carboxymethyllysine (CML) and N^{ϵ} -carboxyethyllysine (CEL), formed by glycation from GO and MGO, are among the major AGEs in tissue proteins. Incubation with GO or MGO resulted in higher CML and CEL formation in the two cysteine residues containing α A-crystallin (α AC) than in the cysteine lacking α B-crystallin (α BC). Mass spectrometric data showed K70 and K166 to be heavily modified with CML and CEL in GO- and MGO-modified α AC. *In silico* analysis of the structure of α AC showed K70 and K166 to be proximal to C142. Mutation or reductive alkylation of cysteine residues in α AC significantly reduced CML and CEL formation. The addition of GSH or *N*-acetylcysteine enhanced CML and CEL formation in α BC. The introduction of a cysteine residue proximal to a lysine residue in α BC increased the CML and CEL accumulation. Our data showed that CML and CEL formation occurs through a hemithioacetal intermediate formed from the reaction between thiols and GO or MGO. Together, these results highlight a mechanism by which thiols influence protein AGE levels. In addition, CML and CEL are ligands for RAGE, a receptor for AGEs, which has been implicated in several aging and diabetes-associated diseases. Therefore, further understanding of the biosynthesis of CML and CEL could lead to the development of new therapies against those diseases.

Advanced glycation end product (AGE) formation represents a major chemical modification in biological macromolecules, including proteins, lipoproteins, and nucleic acids (1). AGEs are formed through the nonenzymatic reaction of the carbonyl group of sugars and carbonyl compounds with the amino group of lysine and arginine residues in proteins (2, 3). Glucose, fructose, and ribose are the major sugars that form AGEs in proteins *in vivo* (4, 5). Ascorbate oxidation products

are another source (6, 7). However, the α -dicarbonyl compounds, glyoxal (GO) and methylglyoxal (MGO), are the dominant precursors of AGEs (8–10). These carbonyls are formed through metabolic pathways, fragmentation of sugars, degradation of Maillard reaction intermediates, ascorbate oxidation, and lipid peroxidation (8, 11).

GO and MGO react with lysine residues to form AGEs, such as N^{ϵ} -carboxymethyllysine (CML) and N^{ϵ} -carboxyethyllysine (CEL) (8, 12). They also react with the guanidino group of arginine residues to form dihydroxyimidazolidine and N^7 -carboxymethylarginine (from GO), and hydroimidazolones MG-H1, MG-H3, and N^7 -carboxyethylarginine (from MGO) (13–15). Amino acid crosslinking AGEs, such as pentosidine and glucosepane, are formed between lysine and arginine residues, and glyoxal lysine-dimer (GOLD) and methylglyoxal lysine-dimer (MOLD) are formed between two lysine residues (14, 16). Regardless of how they are formed, AGEs cause structural and functional changes in proteins that have pathological implications for aging and diabetes-associated diseases. Several studies have shown that extracellular AGEs exert biological activity by engaging with a cellular receptor known as RAGE (receptor for AGEs; (17)). Previous work has linked AGE formation in tissue proteins to aging and diabetic complications (14, 18). Several methods to prevent AGE formation and reverse AGEs have been attempted (19, 20), but none have been successful in human clinical trials (19–21).

Human lens proteins have negligible turnover throughout an individual's life and, therefore, accumulate chemical modifications from oxidation, glycation, deamidation, and kynurenine- and dehydroalanine-mediated modifications during aging (22–24). Some modifications are more prevalent in cataractous lenses (24), implicating them in cataract formation. The lens contains high levels of reduced GSH (25), which helps protect proteins from oxidative damage. GSH also inhibits ascorbate oxidation and prevents AGE formation from ascorbate oxidation products (26). However, as the lens ages, it loses GSH, and its antioxidative enzymes decrease (27), leading to increased oxidative and glycation-mediated damage. Several studies have reported AGEs in human lenses (28). Prior research has shown the progressive accumulation of AGEs in

* For correspondence: Sudipta Panja, sudipta.panja@cuanschultz.edu; Ram H. Nagaraj, ram.nagaraj@cuanschultz.edu.

Proximal cysteine residues facilitate N^ε-carboxyalkylation

human lenses with age and accelerated accumulation in cataractous lenses (29). Our previous study has demonstrated a strong correlation between the stiffness of the lens and AGEs in lens proteins, suggesting a potential role for AGEs in presbyopia (16). Furthermore, we have shown that carboxitin, a chimeric compound consisting of mercaptoethylguanidine linked through a disulfide bond to GSH diethyl ester, inhibits AGE formation and supplies GSH to the lens and can reduce lens stiffness (30), providing additional evidence for a role for AGEs in lens aging and presbyopia.

CML in lens proteins is derived from glycation by GO, ascorbate oxidation products (31, 32), and products of glucose auto-oxidation (33). On the other hand, CEL is exclusively produced from MGO. Previous studies revealed that adding cysteine enhanced CML formation from GO in proteins (34, 35). The authors proposed that free thiol in cysteine stabilizes the lysine-GO adduct and facilitates CML formation. However, cysteine is likely more reactive than lysine for nucleophilic addition with GO under physiological conditions. Based on this, we hypothesized that the thiols could facilitate N^ε-carboxyalkylation of lysine residues by α -dicarbonyls in proteins through a hemithioacetal intermediate, much like the acylation of lysine residues facilitated by the S \rightarrow N transfer of an acetyl group from a thioester to lysine residues (36). In this study, we present evidence for thiol-mediated enhancement of CML and CEL formation in proteins. We propose that this mechanism may have implications not only for lens proteins but also for other cellular and extracellular proteins prone to CML and CEL modifications during aging and under disease conditions.

Results

α A-crystallin accumulates more AGEs than α B-crystallin and γ S-crystallin

To determine the role of cysteine residues in CML and CEL formation, α A-crystallin (α AC), α B-crystallin (α BC), or γ S-crystallin (γ SC) (2 mg/ml, each) were incubated with GO or MGO (500 μ M) for 3 days under physiological conditions. LC-MS/MS analysis indicated that α AC is highly modified with CML and CEL (Fig. 1, A and B). Results indicated a 5.5- and 1.6-fold higher CML content in α AC compared with α BC and γ SC (Fig. 1A). CEL accumulation in these proteins showed a similar trend of 7.1- and 2.5-fold higher levels in α AC compared with α BC and γ SC (Fig. 1B). The levels of CEL were lower than CML, possibly because of MGO being less reactive than GO. We also determined the levels of lysine-lysine crosslinking AGEs, GOLD and MOLD (Fig. S1). The levels were not significantly different between α AC and α BC. The monoarginine modifications, G-H3 (sum of GO-dihydroxyimidazolidine and N⁷-carboxymethyl arginine after acid hydrolysis), MG-H3, and MG-H1, were also similar between α AC and α BC (Fig. S2). The MOLD levels in γ SC were significantly lower than α AC and α BC (Fig. S1), and MG-H3 levels in γ SC were significantly higher than α AC (Fig. S2). CML and CEL levels were also measured in α AC, α BC, and γ SC after incubation with GO and MGO in PBS (Fig. S3).

Results indicated a similar increase in CML and CEL content in α AC compared with α BC and γ SC. Glycolaldehyde (GA) is one of the precursors for the formation of CML. GA-incubated α AC forms higher levels of CML than α BC and γ SC, similar to GO (Fig. S4). Together, these results demonstrated that only CML and CEL, but not the lysine-lysine crosslinking AGEs or hydroimidazolones, are affected by the proximal cysteine residues in proteins.

Hotspots for CML and CEL formation in α AC

To determine whether a particular lysine residue in proteins is more susceptible to CML formation than others in proteins, we first determined the conditions that lead to minimal CML modification in α AC by altering the concentrations of GO and the length of time for incubation. We found high levels of CML in α AC after 3 days (at a concentration of 3 mg/ml) incubated with 750 μ M of GO (Fig. S5). Hence, we opted for a 3-day incubation period and varied the concentration of GO to identify a concentration that produces minimal CML modification (0–750 μ M). By LC-MS/MS, we observed that α AC treated with 75 μ M of GO produced minimal CML modification. This sample was used to detect hotspots for CML modification. We replicated these conditions to modify α AC with MGO to identify the CEL hotspots. By mass spectral analysis, we identified five lysine residues, K70, K78, K88, K99, and K166, which displayed CML and CEL modifications in α AC (Table 1). A comparison of the peak area of GO- or MGO-treated samples with the untreated control samples revealed that CML and CEL modifications at K70 and K166 were higher than at other lysine residues. Intriguingly, the positions of K70 and K166 are proximal to a cysteine residue C142 in α AC. These data suggested that a cysteine residue proximal to lysine residues promotes the formation of CML and CEL in α AC.

In silico modeling shows the proximity of cysteine residues to lysine residues

α BC and α AC contain 10 and 7 lysine residues, respectively (Fig. 1, C and D). α BC does not contain cysteine residues, whereas α AC contains two free cysteine residues at 131 and 142. Figure 1D shows the 3D structure of α AC where K70 and 166 are in close proximity to C142 at 5.18 and 3.16 Å distances, respectively. These data suggested that a distance within 6 Å between cysteine and lysine residues is conducive to the thiol-mediated CML and CEL formation in α AC. Figure 1E shows the 3D crystal structure of γ SC, where none of the cysteine residues are within the 6 Å distance of a lysine residue; all were at >9 Å distance, which suggested why γ SC did not favor CML formation as much as α AC, despite containing 7 cysteine and 10 lysine residues.

Reductive alkylation of cysteine residues of α AC reduces CML and CEL formation

We further investigated the impact of cysteine on N^ε-carboxyalkylation of α AC. To block the cysteine residues, we

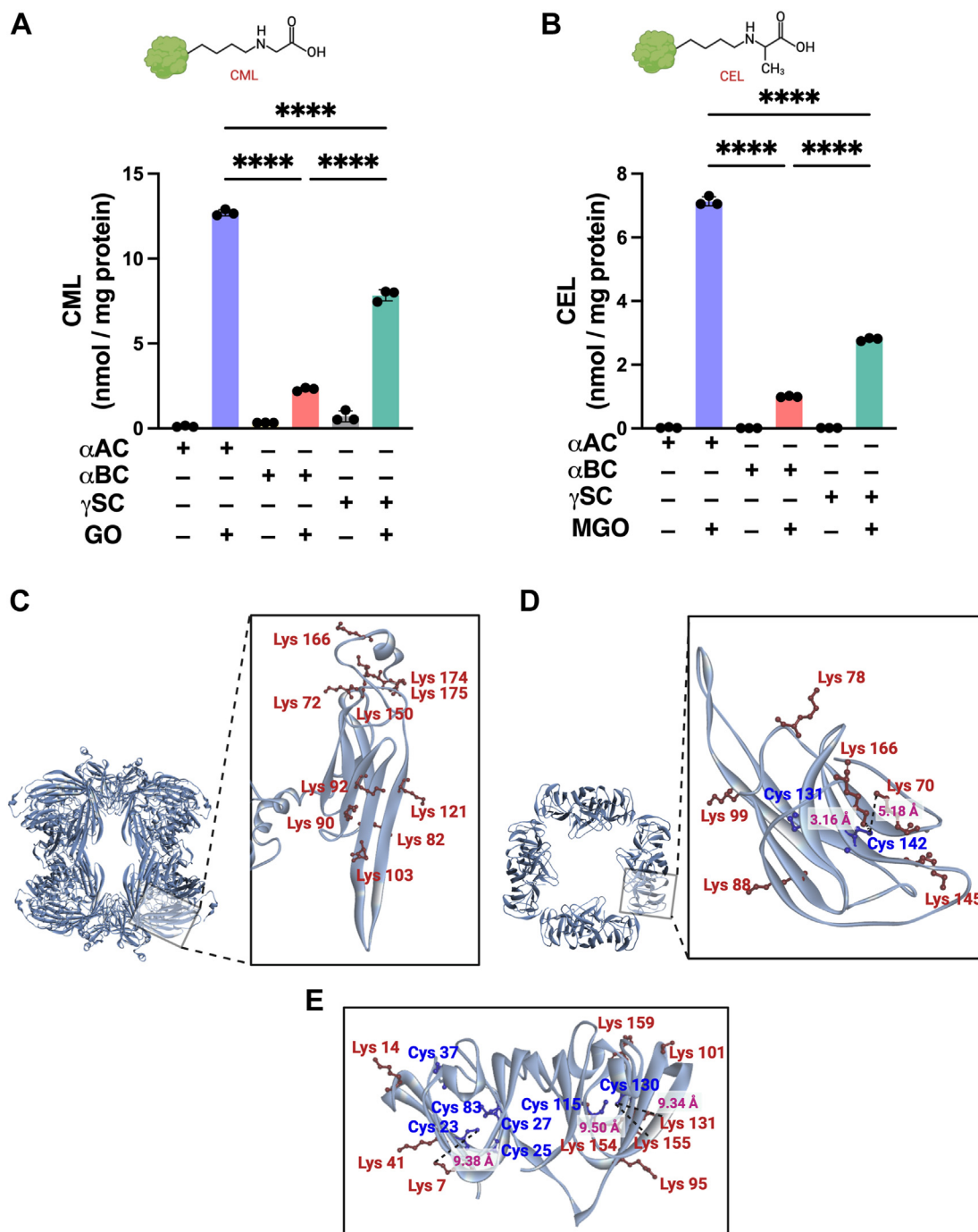


Figure 1. CML and CEL formation is higher in α AC than in α BC or γ SC. Human recombinant α AC, α BC, and γ SC (2 mg/ml) were incubated with or without GO (500 μ M) or MGO (500 μ M) for 3 days at 37 °C. The proteins were dialyzed, acid hydrolyzed, and subjected to CML (A) and CEL (B) analysis by LC-MS/MS. *In silico* modeling shows the positions of lysine residues in α BC (PDB ID: 2YGD; C) and the proximity of cysteine and lysine residues in α AC (PDB ID: 6T1R; D) and γ SC (PDB ID: 6T1R; E). The bar graphs represent the mean \pm SD of three independent experiments. **** p < 0.0001. α AC, α A-crystallin; α BC, α B-crystallin; CEL, N^ε-carboxyethyllysine; CML, N^ε-carboxymethyllysine; GO, glyoxal; MGO, methylglyoxal; PDB, Protein Data Bank; γ SC, γ S-crystallin.

reduced disulfides in α AC by treating with Tris(2-carboxyethyl)phosphine hydrochloride (TCEP) and DTT and then alkylated cysteine residues with N-ethyl maleimide (NEM). We confirmed the blocking of cysteine residues by comparing the level of free thiols before and after RA (Fig. 2A). The results showed a significant decrease in free thiols after RA (p < 0.0001). 2,4,6-Trinitrobenzenesulfonic acid (TNBS) assay result confirmed that NEM did not

react with lysine residues (Fig. 2B). To compare the reactivity of GO or MGO toward RA and control α AC, we performed LC-MS/MS analysis, and the results showed that RA of α AC resulted in a 4.2- and 3.1-fold decrease in the formation of CML and CEL, compared with control α AC (Fig. 2, C and D). These results further supported that cysteine residues promote N^ε-carboxyalkylation by α -dicarbonyls in α AC. Based on these results, we propose that an

Proximal cysteine residues facilitate N^ε-carboxyalkylation

Table 1
K70 and 166 in αAC are the hotspots for CML and CEL formation

Modification	Lysine site	Number of peptides	EIC intensity			Fold change	
			Control	GO	MGO	GO/control	MGO/control
CML	K70	5	2.37E + 06	7.14E + 07	4.51E + 06	30.13	1.90
	K78	1	1.86E + 06	3.40E + 06	5.89E + 06	1.83	3.17
	K88	2	3.49E + 06	6.52E + 06	9.93E + 06	1.87	2.84
	K99	3	1.44E + 07	2.40E + 07	2.15E + 07	1.66	1.49
	K166	4	9.99E + 06	2.68E + 08	9.48E + 06	26.81	0.95
CEL	K70	6	6.64E + 05	0.00E + 00	8.53E + 07	0.00	128.45
	K78	1	0.00E + 00	0.00E + 00	3.33E + 06	ND	
	K88	1	0.00E + 00	0.00E + 00	1.86E + 06	ND	
	K99	1	0.00E + 00	0.00E + 00	1.20E + 06	ND	
	K166	5	0.00E + 00	0.00E + 00	7.31E + 07	ND	

Extracted ion chromatogram (EIC) intensities were summed per lysine site basis in control, GO- and MGO-treated αAC samples. Based on a fold-change analysis, K70 and 166 in αAC were identified as the hotspots for CML formation with 30.13- and 26.81-fold changes, respectively. The summed peptide intensities for CEL formation on K70 and 166 were at least an order of magnitude higher than other lysine sites.

Abbreviation: ND, not determined.

S→N transfer of a C-2- or C-3-based reactive intermediate formed on cysteine residues is transferred to the ε-amino group of lysine residue to form CML and CEL.

C142A mutation in αAC reduced the levels of CML and CEL

To determine the role of spatial proximity of cysteine residues in promoting N^ε-carboxyalkylation in αAC, we mutated C131 and C142 to C131A and C142A (Fig. 3, A and B). We also generated a double mutant C131AC142A (Fig. 3C). These mutations had minimal impact on the secondary and tertiary structure of αAC, as evident from CD and fluorescence studies (Fig. S6). Upon incubation of these mutant proteins along with WT protein, followed by LC-MS/MS analyses, we observed a substantial reduction in the CML (2.5- and 3.8-fold) and CEL (2.4- and 2.7-fold) levels in C142A and C131AC142A αAC mutant proteins (Fig. 3, D and E). Conversely, the single mutant C131A exhibited a comparable accumulation of CML and CEL to that of the WT αAC. Structural examination revealed the spatial proximity of C142 to K70 (5.2 Å) and K166 (3.2 Å). These observations suggested that C142 is the site where an S→N from C-2 or C-3 carbon to K70 and K166 occurred in αAC, leading to N^ε-carboxyalkylation.

External thiols increase the CML and CEL levels in αBC

We anticipated that adding GSH or N-acetylcysteine (NAC) would promote CML and CEL formation in αBC by transferring the reactive intermediate group from cysteine to lysine. LC-MS/MS analysis results showed a notable increase in CML and CEL levels in αBC upon treatment of GSH or NAC along with GO or MGO (Fig. 4, A and B). Results also indicated that NAC increased CML and CEL formation by 1.7- and 1.9-fold more than GSH. The higher reactivity of the thiol group in NAC likely facilitates more efficient S→N transfer reactions, thereby enhancing the CML and CEL formation in lysine residues of αBC. However, the addition of GSSG in the place of GSH did not alter the CML levels (Fig. S7). These results suggested that external thiols have a role in elevating CML and CEL formation.

Introduction of a cysteine residue proximal to a lysine residue increases the CML and CEL levels in αBC

We employed site-directed mutagenesis to strategically introduce cysteine residues adjacent to lysine residues in αBC to understand the S→N transfer mechanism. This approach enabled us to explore the potential impact of proximal cysteines on N^ε-carboxyalkylation. We generated three αBC mutants: K92C, V169C, and E99C. *In silico* structural analysis showed distances between the introduced cysteine and lysine residues (Fig. 5, A–C). In the K92C mutant, the distance between C92 and K90 was 5.0 Å, whereas in the V169C mutant, it was 2.9 Å between C169 and K150. In the E99C mutant, the distance between C99 and K92 was 4.8 Å. After incubating these mutant proteins with GO and MGO, we measured the CML and CEL levels by LC-MS/MS. The K92C mutant of αBC exhibited significantly ($p < 0.0001$) higher levels of CML and CEL compared with WT-αBC (Fig. 5, D and E). However, we observed no increase in CML and CEL levels in the V169C and E99C mutants compared with WT αBC. In the K92C mutant, C92 is separated from K90 by two peptide bonds. However, in mutants V169C and E99C, the proximity of C169 and K150, and C99 and K92, is likely determined by the folding of the protein's secondary structure, and therefore, changes in structural dynamics and spatial orientation of the protein folding may have resulted in an increase in the distance between lysine and cysteine residues.

Distance between cysteine and lysine dictates CML and CEL formation

To further understand the effects of the proximity of cysteine and lysine residues in forming CML and CEL, we investigated five peptides with varying distances between cysteine and lysine (Fig. 6A). All peptides (1 mg/ml) were incubated with 100 μM GO or 500 μM MGO for 3 days at pH 7.4 in 100 mM sodium phosphate buffer at 37 °C. LC-MS/MS analysis revealed a similar accumulation of CML and CEL among these peptides (Fig. 6, B and C). The amount of CML or CEL was lowest when cysteine and lysine were next to each other, possibly because the side chain of these residues could occupy opposite planes of the peptide bond. Interestingly, the

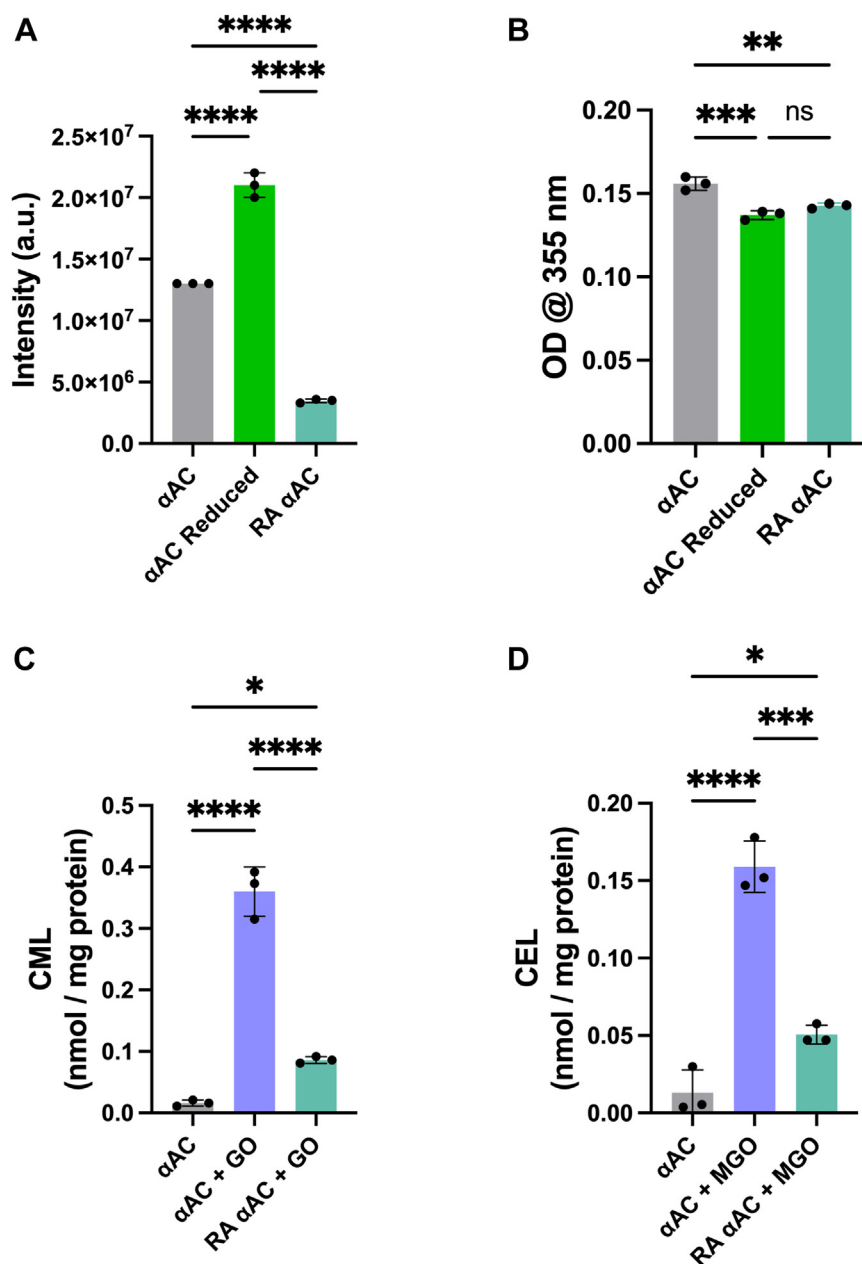


Figure 2. Reductive alkylation (RA) of cysteine residues in α AC reduces CML and CEL formation. Cysteine residues of α AC were reductively alkylated in the presence of DTT and NEM. Free thiol fluorescence (A) and free amine levels (B) were quantified in reduced and reductively alkylated (RA) α AC. Reduced and RA α AC (2 mg/ml) were incubated with GO (500 μ M) or MGO (500 μ M) for 3 days at 37 °C. The proteins were dialyzed, acid hydrolyzed, and subjected to CML (C) and CEL (D) analysis by LC-MS/MS. The bar graphs represent the mean \pm SD of three independent experiments. * p < 0.05, ** p < 0.01, *** p < 0.001, and **** p < 0.0001. α AC, α A-crystallin; CEL, N^ε-carboxyethyllysine; CML, N^ε-carboxymethyllysine; GO, glyoxal; MGO, methylglyoxal; NEM, N-ethyl maleimide.

levels of CML and CEL were highest when there was an alanine between cysteine and lysine, about 7.6 Å apart. As the distance increased from one to six amino acid residues, the formation of CML and CEL progressively decreased. These results indicated that the distance between cysteine and lysine significantly affects the formation of AGEs.

We investigated the significance of the distance between C and K residues in the formation of CML in proteins from HUVEC cells (incubated with GO) with high CML modifications, as reported by Di Sanzo *et al.* (37). We specifically

focused on proteins with at least six CML modifications and assumed a proximity distance of 15 Å between C and K to favor CML formation. The results, presented in Table S1, revealed that while some CML-modified K residues were within 15 Å from C residues, others were not. In one protein, myosin-9, none of the CML-modified K residues were proximal to C residues. These findings suggested that while CML formation may occur through proximal cysteine residues, there are also additional mechanisms at play, potentially involving protein-free thiols.

Proximal cysteine residues facilitate N^ε-carboxyalkylation

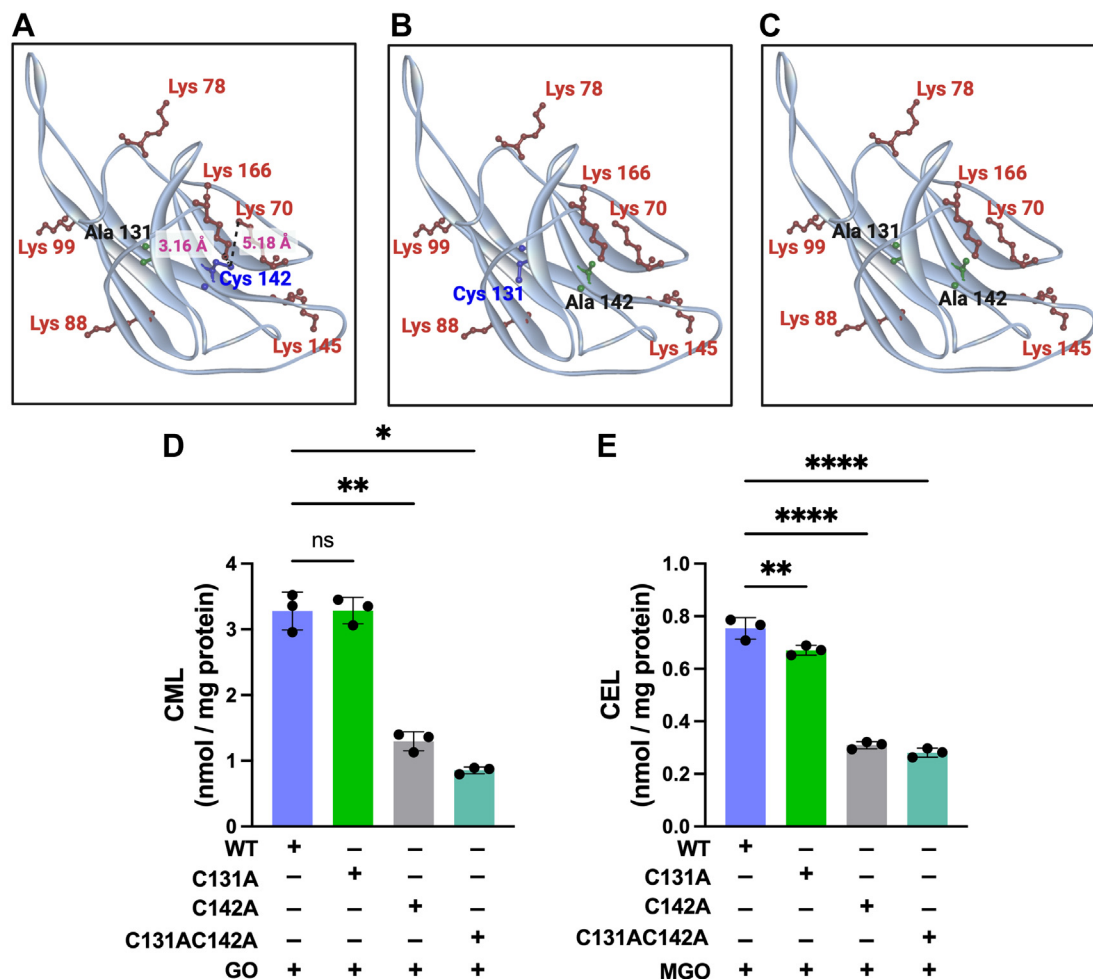


Figure 3. Mutation of C142 to A142 in α AC reduced CML and CEL formation. *In silico* modeling shows lysine and cysteine residues in α AC-C131A (A), α AC-C142A (B), α AC-C131A/C142A (C). WT α AC and mutant α AC (2 mg/ml, each) were incubated with GO (500 μ M) or MGO (500 μ M) for 3 days at 37 $^{\circ}$ C. After incubation, the proteins were dialyzed, acid hydrolyzed, and subjected to CML (D) and CEL (E) analysis by LC-MS/MS. The bar graphs represent the mean \pm SD of two to three independent experiments. * p < 0.05, ** p < 0.01, **** p < 0.0001, ns, not significant. α AC, α A-crystallin; CEL, N^ε-carboxyethyllysine; CML, N^ε-carboxymethyllysine; GO, glyoxal; MGO, methylglyoxal.

CML is formed through a hemithioacetal intermediate

GO and MGO react spontaneously with GSH and NAC to form a reversible hemithioacetal (Figs. 7A and S8). Glyoxalase I (GLO1) uses this as a substrate and converts it to S-2-hydroxyacylglutathione, which is then converted to an aldinate by glyoxalase II (38). To determine whether the hemithioacetal is an intermediate in the thiol-enhanced CML formation, we incubated GSH with GO in the presence and absence of GLO1 and monitored absorbance at 290 nm for hemithioacetal formation. Hemithioacetal formation occurred rapidly, saturating at \sim 25 min (Fig. 7A). However, in the presence of recombinant human GLO1, the hemithioacetal levels were minimal, suggesting that GLO1 effectively catalyzed the conversion of hemithioacetal to S-2-hydroxyacylglutathione. With the heat-inactivated GLO1, the hemithioacetal levels were similar to those observed in the absence of GLO1 (65 $^{\circ}$ C, for 3 min). We added *t*-Boc-lysine (Boc-Lys) to a 50-min preincubated mixture of GSH and GO in the presence and absence of GLO1 or heat-inactivated

GLO1 and incubated further for up to 2 days. We then determined the levels of CML by LC-MS/MS in these incubation mixtures. After 1 and 2 days of incubation, CML levels were higher in the GSH + GO + Boc-Lys sample (Fig. 7B) than in GSH + GO + Boc-Lys + GLO1 and GO + Boc-Lys samples. However, in the GSH + GO + Boc-Lys + GLO1 (heat-inactivated) sample, the CML levels were slightly higher. To determine whether GLO1 can reduce CML formation in proteins, a mixture of GSH and GO was incubated for 3 days with α AC in the presence and absence of GLO1 and heat-inactivated GLO1. Results suggested that GLO1 significantly (p < 0.0001) reduced the GO-mediated formation of CML compared with heat-inactivated GLO1 (Fig. 7C). Furthermore, the active, but not the inactive, GLO1 decreased the GSH-enhanced CML formation in α BC (Fig. S9). Together, these data suggested that hemithioacetal is an important intermediate in CML formation. Moreover, we varied the GSH concentration from 0 to 2 mM and measured the CML levels in α BC incubated with GO (500 μ M) for 3 days (Fig. S10). The

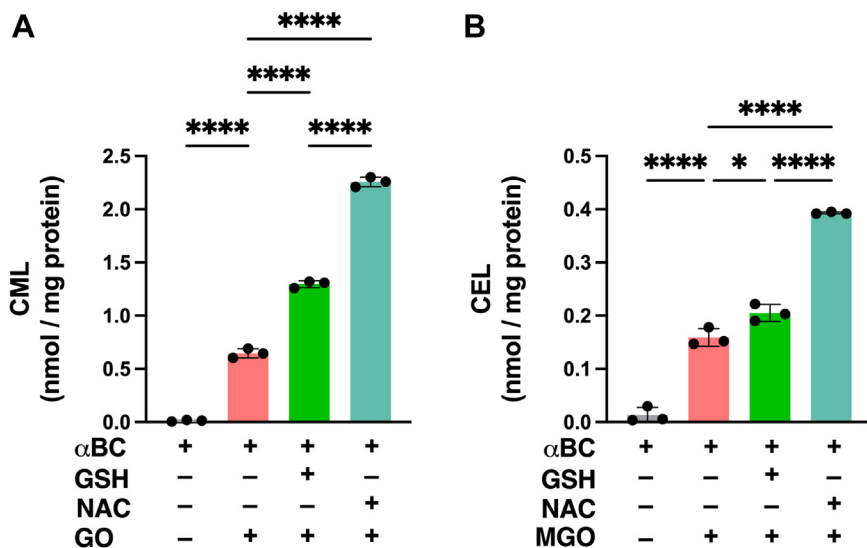


Figure 4. External thiols increase the CML and CEL formation in αBC. αBC (2 mg/ml) was incubated with GO (500 μM) or MGO (500 μM) in the presence of GSH or NAC (500 μM) for 3 days at 37 °C. Proteins were dialyzed, acid hydrolyzed, and subjected to CML (A) and CEL (B) analysis by LC-MS/MS. The bar graphs represent the mean ± SD of three independent experiments. **p* < 0.05, *****p* < 0.0001. αBC, αB-crystallin; CEL, N^ε-carboxyethyllysine; CML, N^ε-carboxymethyllysine; GO, glyoxal; MGO, methylglyoxal; NAC, N-acetylcysteine.

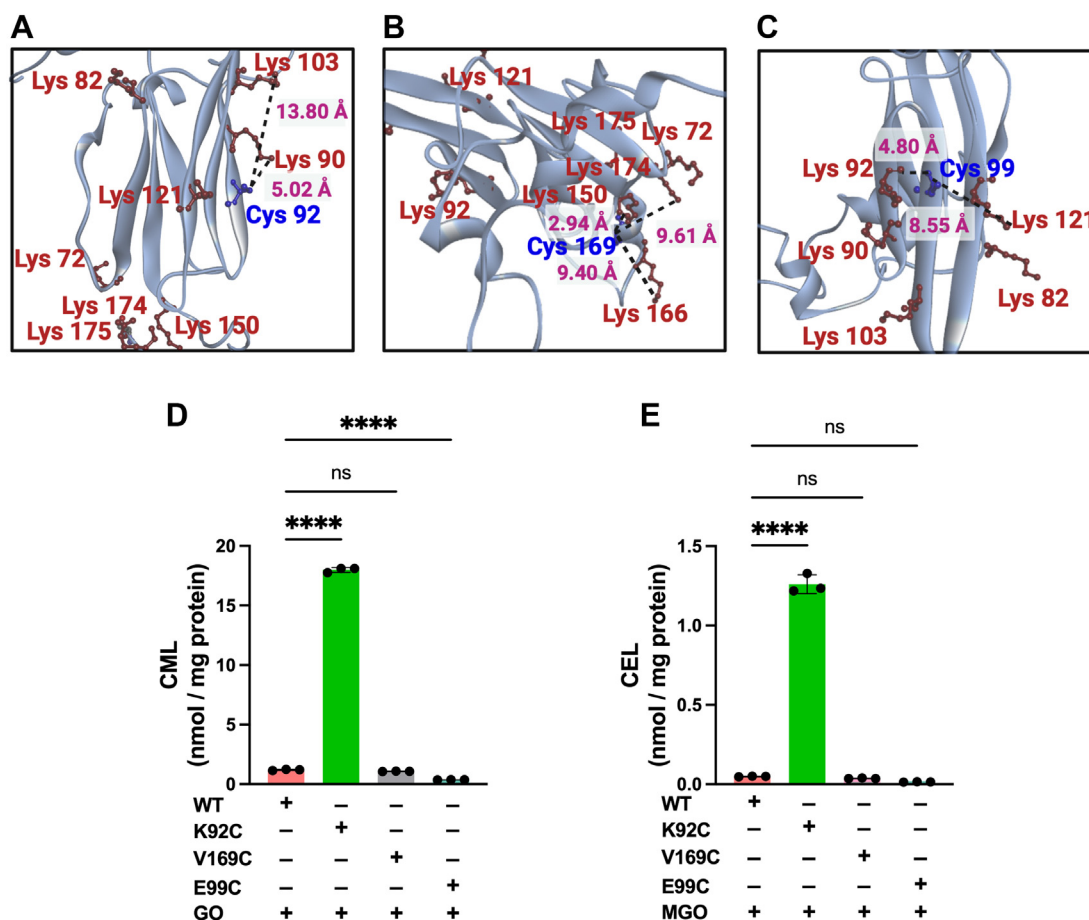


Figure 5. Introduction of a cysteine residue proximal to lysine residue increases CML and CEL levels in αBC. *In silico* modeling shows the proximity of lysine and cysteine residues in αBC-K92C (A), αBC-V169C (B), and αBC-E99C (C). Mutated and WT-αBC (2 mg/ml) was incubated with GO (500 μM) or MGO (500 μM) for 3 days at 37 °C. Proteins were dialyzed, acid hydrolyzed, and subjected to CML (D) and CEL (E) analysis by LC-MS/MS. The bar graphs represent the mean ± SD of three independent experiments. *****p* < 0.0001, ns, not significant. αBC, αB-crystallin; CEL, N^ε-carboxyethyllysine; CML, N^ε-carboxymethyllysine; GO, glyoxal; MGO, methylglyoxal.

Proximal cysteine residues facilitate N^ε-carboxyalkylation

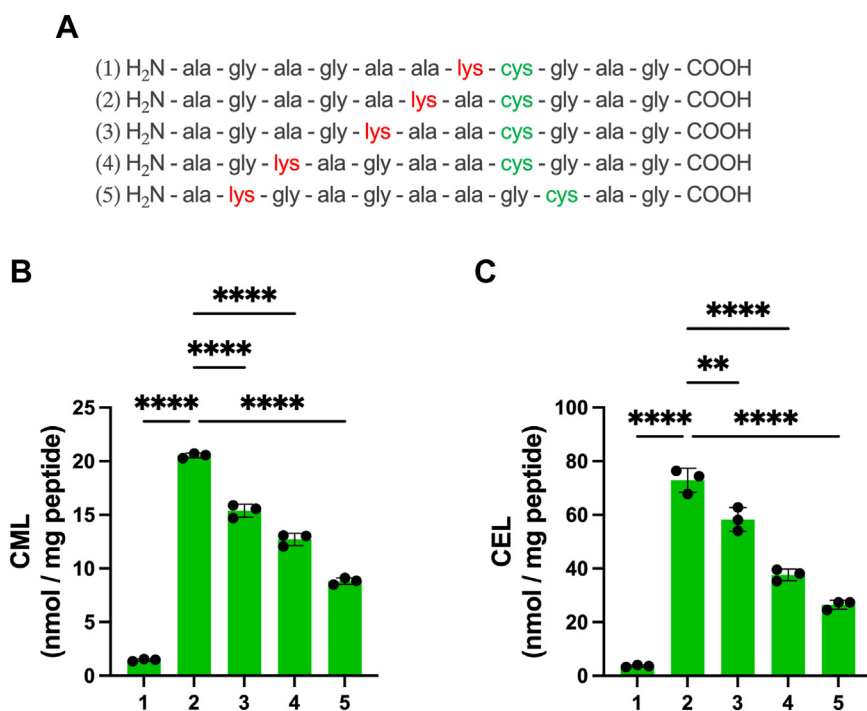


Figure 6. Distance between cysteine and lysine affects CML and CEL formation. Amino acid sequence of five peptides with differences in cysteine–lysine distances (A). The peptide (1 mg/ml) was incubated with or without GO (100 μ M) or MGO (500 μ M) for 3 days at 37 °C. Peptides were acid hydrolyzed and subjected to CML (B) and CEL (C) analysis by LC–MS/MS. ** p < 0.01, **** p < 0.0001. CEL, N^ε-carboxyethyllysine; CML, N^ε-carboxymethyllysine; GO, glyoxal; MGO, methylglyoxal.

results demonstrated that an increase in GSH concentration (from 250 to 500 μ M) led to greater CML synthesis in α BC. When the GSH levels were increased to 1 and 2 mM, there was no appreciable further increase in the levels of CML. Together, our results suggested that hemithioacetal, formed from GSH, promotes CML formation in proteins. In addition, the thiol-catalyzed CML formation was not observed in ribose or glucose-glycated α BC (Fig. S11). These results further reiterated the requirement of a hemithioacetal intermediate in thiol-catalyzed CML formation.

Reductive alkylation of cysteine residues of cytochrome c and hemoglobin reduces CML and CEL formation

Cytochrome *c* (Cyt *c*) and hemoglobin (Hgb) were used as additional proteins to investigate the impact of cysteine on carboxyalkylation of lysine. Cyt *c* contains two cysteine residues at positions 14 and 17. There are 19 lysine residues. Several cysteine and lysine residues in this protein are within 15 Å distance from each other; for example, the distance between cysteine 14 and lysine 13 is approximately 7.8 Å. The Hgb subunit beta contains one cysteine residue (C93), and in three instances, this cysteine is proximal to a lysine residue in the same chain (<15 Å). Reductive alkylation (RA) of cysteine residues in these proteins significantly reduced thiol levels but had no effect on lysine residues (Fig. S12, A and B). Results indicated that RA reduced CML and CEL levels in both Cyt *c* and Hgb (Fig. S12, C and D), reiterating the requirement of free thiols for the promotion of N^ε-carboxyalkylation by α -dicarbonyls in proteins.

Formation of CML and CEL is preferred over acetylation of lysine

To determine whether CML and CEL formation is preferred over acetylation of lysine (AcK) formation in proteins, 1 mg/ml of α AC and α BC was treated with 500 μ M GO or MGO in the presence or the absence of 500 μ M acetyl CoA (AcCoA). Following a 3-day incubation, we conducted LC–MS/MS analysis to determine the impact of AcCoA on CML and CEL accumulation. Our results revealed that adding AcCoA does not significantly affect the CML and CEL levels either in α AC or α BC (Fig. 8, A–D). These results suggested that when exposed to competing reactants, α -dicarbonyls and AcCoA, which is likely *in vivo*, CML and CEL formation appears to be independent of AcK formation.

Discussion

The purpose of this study was to investigate the mechanisms by which thiols influence the α -dicarbonyl-mediated N^ε-carboxyalkylation in proteins. Through various approaches, we have confirmed that cysteine residues in close proximity to lysine residues promote the formation of CML and CEL in proteins. First, our results showed that the formation of CML and CEL is higher in α AC compared with α BC. This difference is due to the absence of cysteine in α BC and the proximity of K70 and K166 to C142 in α AC. Second, a decreased formation of CML and CEL in α AC was observed when cysteine residues were reductively alkylated. Third, the mutation of C142 to alanine led to a significant decrease in CML and CEL formation in α AC, and fourth, the introduction of cysteine residues

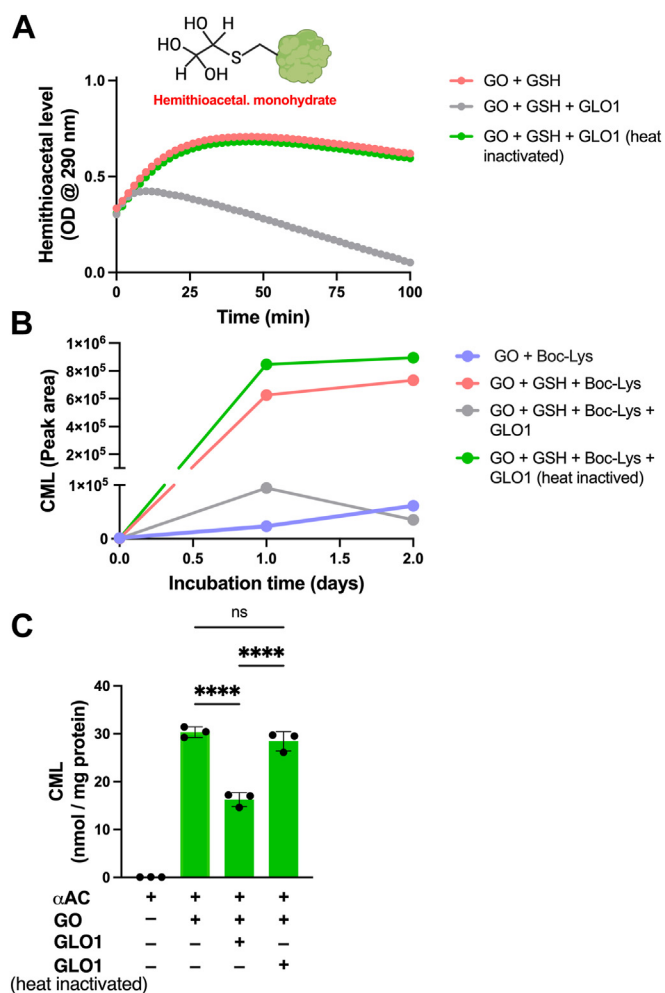


Figure 7. Hemithioacetal is the key intermediate in thiol-mediated CML formation. The formation of hemithioacetal was monitored by measuring absorbance at 290 nm in the incubation mixture containing GO (5 mM) with GSH (5 mM) in 100 mM sodium phosphate buffer, pH 7.4 at room temperature (A). The addition of GLO1 (5 μ g) dramatically reduced hemithioacetal levels. Native GLO1 or heat-inactivated GLO1 was added to 50-min GO + GSH-incubated samples. t-Boc-lysine (t-Boc-Lys; 5 mM) was added to 50-min GO + GSH-incubated samples in the presence of native or heat-inactivated GLO1, and the mixtures were incubated for up to 2 days. CML levels measured by LC-MS/MS after acid hydrolysis of the mixtures showed a substantial increase in CML formation by the addition of t-Boc-Lys and a significant inhibition of CML formation upon the addition of native but not heat-inactivated GLO1 (B). α AC (2 mg/ml) was incubated with GO (500 μ M) in the presence and absence of GLO1 for 3 days at 37 $^{\circ}$ C. Heat-inactivated GLO1 was used as the control. Proteins were dialyzed, acid hydrolyzed, and subjected to CML analysis by LC-MS/MS (C). **** p < 0.0001, ns, not significant. α AC, α A-crystallin; CML, N^ε-carboxymethyllysine; GLO1, glyoxalase I; GO, glyoxal.

proximal to K92 in α BC led to enhanced formation of CML and CEL in α BC. These observations suggest that cysteine residues in close proximity to lysine residues promote N^ε-carboxyalkylation by α -dicarbonyl compounds through an S \rightarrow N transfer mechanism.

Interestingly, the formation of hydroimidazolones, which are arginine modifications by GO and MGO, was not affected. Therefore, the observed effects are restricted to glycation of lysine residues. One caveat to this principle is that it only applies to N^ε-carboxyalkylation. The formation of GOLD and MOLD, which are lysine modifications by GO

and MGO, were unaffected by the proximal cysteine residues. The apparent restrictive effect can be explained as follows: the formation of CML and CEL involves a nucleophilic attack by the thiol group of cysteine on the carbonyl functions of α -dicarbonyls, forming a hemithioacetal intermediate. Subsequent nucleophilic substitution and elimination of cysteine by the ϵ -lysine function lead to the transfer of the reactive hemiacetal group of the former α -dicarbonyl to lysine as S \rightarrow N transfer (probably through a hemiaminal intermediate), resulting after rearrangement in the formation of CML or CEL (Fig. 9). This mechanism is in line with the well-established tautomeric isomerization during the synthesis of amide-AGEs, such as glycolic acid lysine amide, glyoxal-lysine-amide-crosslink and amidine-AGE, glyoxal amidine crosslink (39, 40). The catalytic effect of cysteine takes into account both the potent nucleophilic properties of thiols as well as their excellent leaving qualities in substitution reactions. A more in-depth investigation of the mechanism of the carbonyl isomerization cascade is in progress.

In addition, work on α BC supports hemithioacetal intermediate in CML and CEL formation. α BC does not contain any cysteine residues and, therefore, does not favor CML formation from GO. However, CML formation is substantially increased when GSH or NAC is present along with GO (Figs. 4 and S7). Moreover, GLO1 significantly reduced the GSH-mediated enhancement in CML formation in α BC. Interestingly, when a cysteine residue is introduced at position 92 in α BC, there was a significant increase in the CML formation. These observations suggested the formation of a hemithioacetal intermediate as a key factor in the formation of CML and CEL. In fact, when the hemithioacetal levels were reduced by the addition of GLO1, CML levels were reduced significantly, reiterating the notion that the hemithioacetal, not cysteine or GSH, is the intermediate driving the formation of CML in proteins.

Schwarzenbolz *et al.* (34) described a thiol-dependent increase in CML levels in proteins. In their proposed mechanism (35), they suggested the nucleophilic attack of the Schiff base by cysteine leading to the formation of a hemithioaminal intermediate and its cleavage leading to the formation of CML. However, the potential formation of a more stable hemithioacetal as an intermediate in CML formation was not considered. Further, cysteine is likely more reactive than lysine for nucleophilic addition with GO to form a hemithioacetal under physiological conditions. Our study clearly demonstrated that the hemithioacetal rather than hemithioaminal is an intermediate in thiol-catalyzed N^ε-carboxyalkylation.

Whether proximal cysteine residues affect other AGEs, not investigated in this study, remains unknown. Coukos *et al.* (41) recently reported the formation of mercaptomethylimidazole from the reaction of MGO with proximal cysteine and arginine residues in proteins. They proposed that it was synthesized through a hemithioacetal formed from the reaction between MGO and cysteine. In addition, hemithioacetal formed from the reaction of MGO and thiols is a precursor for lactoyllysine modification in proteins (38). These observations suggest that

Proximal cysteine residues facilitate N^ε-carboxyalkylation

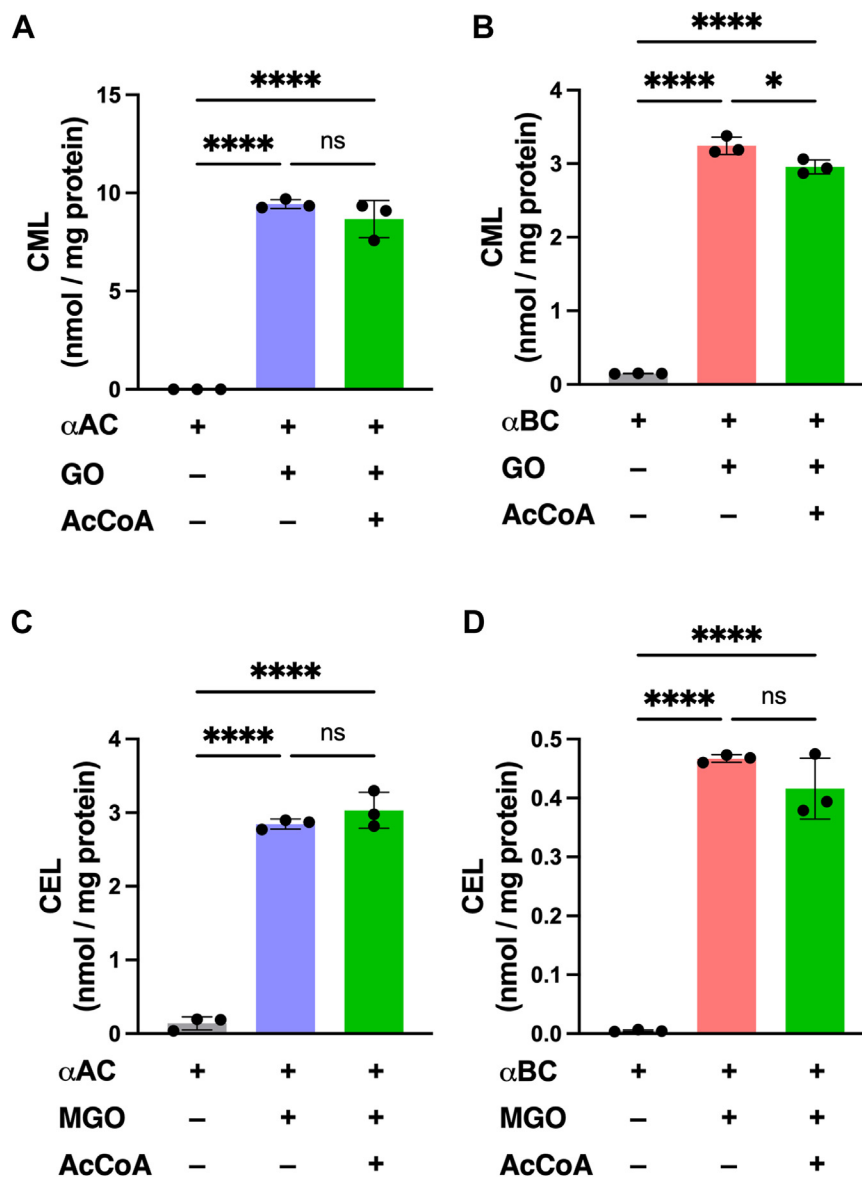


Figure 8. The formation of CML and CEL is independent of lysine acetylation. αAC and αBC (1 mg/ml, each) were incubated with or without AcCoA (500 μM) in the presence of GO or MGO (500 μM) for 3 days at 37 °C. The proteins were dialyzed, acid hydrolyzed, and subjected to CML (A, B) and CEL (C, D) analysis by LC-MS/MS. The bar graphs represent the mean ± SD of two to three independent experiments. **p* < 0.05, *****p* < 0.0001, ns, not significant. αAC, αA-crystallin; AcCoA, acetyl CoA; αBC, αB-crystallin; CEL, N^ε-carboxyethyllysine; CML, N^ε-carboxymethyllysine; GO, glyoxal; MGO, methylglyoxal.

hemithioacetals could play a wider role in protein modifications than previously thought.

The implications of proximal cysteine-mediated N^ε-carboxyalkylation extend beyond the basic biochemical understanding of glycation. Given the link between AGEs and various pathologies, including diabetes-associated complications and neurodegenerative diseases, understanding the molecular mechanisms underlying AGE formation is of utmost clinical relevance. In addition, CML and CEL are the major ligands for RAGE (42, 43), and AGE-RAGE-mediated signaling has been implicated in several diseases associated with aging and diabetes (44, 45). Thus, targeting specific residues or structural motifs that promote AGE-mediated protein modifications could offer novel therapeutic strategies for mitigating AGE-related pathologies. Several compounds,

including guanidine compounds and polyphenols, have been tested for inhibition of AGE formation in tissue proteins. These inhibitors work by scavenging free radicals, chelating metal ions, capturing active carbonyl compounds, and lowering blood glucose levels (46). However, no AGE inhibitor has been developed yet to counteract the hemithioacetal formation, which this study proved to be an important intermediate in CML and CEL formation. In this context, it may be beneficial to increase GLO1 activity through small molecules, as attempted previously (47), enhance GLO1 expression through genetic techniques, or develop more advanced α-dicarbonyl trapping agents to prevent AGE formation from α-dicarbonyls.

AcK is a significant modification in proteins, including lens proteins (48). We recently reported that AcK accumulation in

Proximal cysteine residues facilitate N^ε-carboxyalkylation

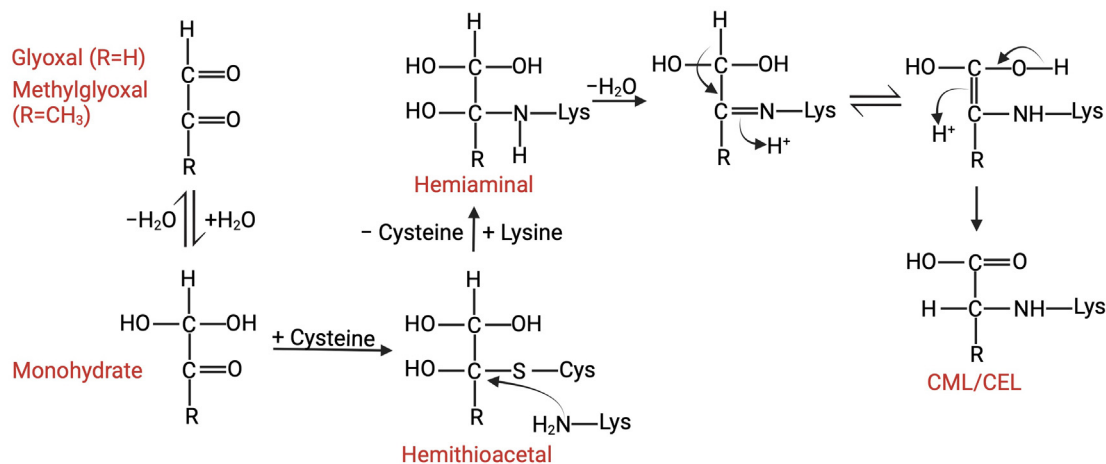


Figure 9. Proposed mechanism of CML and CEL formation via tautomeric isomerization initiated by nucleophilic substitution of a hemithioacetal intermediate by lysine. CEL, N^ε-carboxyethyllysine; CML, N^ε-carboxymethyllysine.

α -crystallin involves the S \rightarrow N transfer of the acetyl group from cysteine to lysine residues (36). Contrary to the S \rightarrow N transfer reported in this study, the mechanism was different and followed by thiol-catalyzed transacylation. This study suggests that thiol-catalyzed CML and CEL formation by tautomeric isomerization is independent of AcCoA-mediated AcK formation in proteins. However, a previous study indicated that prior AcK residue significantly decreases AGE formation in proteins (49). Therefore, further development of acetylating agents, such as aggrelytes (49–51), could have implications for AGE formation in tissue proteins.

Work is underway to discern whether proteins that accumulate high levels of CML during glycoxidative stress have cysteine and lysine residues in close proximity to each other. Whether cysteine oxidation under oxidative stress leads to decreased CML and CEL formation because of the unavailability of the thiol group in cysteine for the S \rightarrow N transfer inducing carboxyalkylation in proteins needs to be investigated. Several lysine residues in serum albumin have been reported to be modified by CML *in vivo* (52). Though CML and CEL can form without the aid of cysteine in proteins, the availability of proximal thiols can greatly enhance their formation. A recent study showed that K233 and K525 in human serum albumin are the main sites where CML is formed (53). These lysine residues are located at a distance of 13.8 and 8.9 Å away from cysteine 265 and 559, respectively, and most of the cysteine residues are oxidized in HSA. The only unoxidized cysteine is at C34, but it is not proximal to K233 or K525. These observations suggest that in HSA, CML and CEL formation might occur through the direct reaction of GO and MGO. We cannot rule out the possibility that cysteine residues in other proteins bound to HSA contribute to CML and CEL formation. Our data showed that CML formation from glucose and ribose in α BC was unaffected by NAC. CML formation from these sugars possibly occurred through oxidative fragmentation of Amadori product (32), which was unaffected by NAC. This notion is supported by the observation that the accumulation of CML in tissues like the human lens increases

with age (16, 54), whereas GSH levels decrease (55). This inverse correlation does not entirely support the thiol-mediated promotion of CML formation; instead, it points to the oxidative fragmentation of Amadori products as a major additional mechanism in CML formation.

The involvement of cysteine in glycation remains poorly documented. For the first time, this study provides new insights into the impact of proximal cysteine residues on lysine, which significantly influences protein glycation, particularly in the formation of CML and CEL. In proteins, the solvent accessibility of cysteine and lysine residues regulates their nucleophilic character (56), thereby potentially affecting their accessibility for glycation. Mechanistically, as an intermediate state, the balance between kinetically favored and thermodynamically stable hemithioacetal formation is the key factor for the glycation process. Under physiological conditions, hemithioacetal formation is kinetically favored but thermodynamically unstable (41, 57). Consequently, proximal lysine may capture the labile alkyl group from cysteine *via* a hemiaminal to form thermodynamically stable N^ε-carboxyalkylated lysine derivatives. However, the availability of cysteine residues for the promotion of N^ε-carboxyalkylation of lysine residues in proteins could be limited by the susceptibility of cysteine residues to oxidation (like in aged human lenses) and other reactions. For example, in the presence of molecular oxygen, proximal cysteine and lysine side chains can form a redox-sensitive nitrogen-oxygen-sulfur bridge (58).

In conclusion, the discovery of proximal cysteine residues as promoters of N^ε-carboxyalkylation of lysine residues by α -dicarbonyl compounds in proteins represents a significant advancement in our understanding of protein chemistry and its implications for health and disease. This phenomenon highlights the intricate interplay of amino acid residues within protein structures and underscores the importance of protein context and conformational dynamics in CML and CEL formation. Furthermore, it offers promising avenues for therapeutic intervention in AGE-related pathologies.

Proximal cysteine residues facilitate N^ε-carboxyalkylation

Experimental procedures

Reagents

GO (catalog no.: 128465), MGO (catalog no.: M0252), GA (catalog no.: G6805), NAC (catalog no.: A7250), GSH (catalog no.: G6529), TCEP (catalog no.: C4706), DTT (catalog no.: D9163), NEM (catalog no.: 23030), AcCoA (catalog no.: A2056), GLO1 (catalog no.: G4252), TNBS (catalog no.: P2297), Cyt *c* (catalog no.: C7752), and Hgb (catalog no.: H2500) were purchased from Sigma–Aldrich. All other chemicals were of analytical grade.

Cloning, expression, and purification of α AC, α BC, γ SC, α AC, and α BC mutants

The genes for proteins were cloned, proteins were expressed in *Escherichia coli*, and purified as previously described (36). Briefly, genes that encode crystallins were synthesized by Twist Bioscience and then inserted into a pET-SUMO expression vector using BamH1 and Xho1 sites. After cloning the genes, they were transformed into *E. coli* BL21 (DE3) cells. A construct for γ SC was encoded in pE-SUMO vector (Addgene plasmid #80753) and was transformed into *E. coli* BL21 (DE3) cells. The plasmids were isolated from the transformed cells using a plasmid miniprep kit from Qiagen, and the sequence was confirmed. The bacterial constructs encoding the proteins were grown in lysogeny broth media at 37 °C. Protein expression was induced using 0.5 mM isopropyl- β ,D-thiogalactopyranoside at a cell density that corresponded to an absorbance 0.6–0.8 at 600 nm. All proteins were expressed in a soluble form and purified using a Ni-Sepharose affinity column from Cytiva. The N-terminal polyhistidine-SUMO tag was removed using Ulp1 protease. Finally, purified proteins were dialyzed in 100 mM phosphate buffer, pH 7.4. The homogeneity of the proteins was confirmed by SDS-PAGE.

Incubation of crystallin with GO and MGO

Human recombinant α AC, α BC, γ SC, mutant α AC, or mutant α BC (1 or 2 mg/ml, each) were incubated for 72 h at 37 °C with or without 500 μ M GO or MGO in 100 mM sodium phosphate buffer, pH 7.4. After incubation, proteins were dialyzed against PBS for 16 h at 4 °C.

Measurement of CML and CEL by LC–MS/MS

Samples were acid hydrolyzed and dried using a previously established protocol (59). The digested samples were then analyzed for AGEs using the LC–MS/MS method with standard addition, as previously described (59). The AGE levels were determined based on the initial protein or peptide concentrations.

Site-specific CML and CEL measurement by LC–MS/MS

One replicate of 10 μ g of control, MGO-treated, and GO-treated human recombinant α AC was prepared using an iST Kit (Preomics), analyzed on an Orbitrap Eclipse with an EZ-Spray Nano source and Ultimate 3000 RSCLnano LC system (Thermo Scientific) as previously described (36). The data

were searched in PEAKS Proteomics Studio, version 10.5. All intensity values were manually checked in FreeStyle software (Thermo Scientific) for quantitation of CML- and CEL-containing peptide hits from the database search using the *m/z* and retention values to confirm the absence or the presence of the modified peptides. Samples were searched against the SwissProt *Homo sapiens* downloaded from UniProt Knowledgebase on July 23, 2023 using a trypsin enzyme search with two missed cleavages allowed, and monoisotopic peptide mass tolerance was set to ± 10.0 ppm and the MS/MS tolerance to ± 0.4 Da since MS/MS spectra were collected in the linear ion trap. The modifications allowed were fixed carbamido-methylation (C) and variable oxidation (M), deamidation (NQ), CML (K, N-Term [58.01 mass shift]), CEL (K, N-term [72.02 mass shift]), MGO-derived hydroimidazolone (R [54.01 mass shift]), and GO-derived hydroimidazolone (R [39.99 mass shift]). Peptides were validated by setting the false discovery rate to 1%, corresponding to a log 10 *p* value score greater than or equal to 30.5 in the dataset. Only peptides containing an internal lysine modification of CML or CEL with an A-Score (modification site score) greater than or equal to 20 were used for site-specific quantitation of CML and CEL modifications.

RA of α AC, Cyt *c*, and Hgb

One milliliter of α AC, Cyt *c*, and Hgb (3 mg/ml, each) was mixed with 5 mM TCEP and 5 mM DTT and incubated at room temperature for 2 h. The protein was dialyzed against 50 mM sodium phosphate buffer, pH 7.0, which was bubbled with N₂ at 4 °C before dialysis. To verify the reduction of α AC, protein-thiol content was measured. Afterward, 600 μ l of 3 mg/ml of reduced α AC, Cyt *c*, and Hgb was alkylated with 2 mM NEM in the dark for 4 h at room temperature. The protein was dialyzed again against 50 mM sodium phosphate buffer, pH 7.0 at 4 °C. Next, α AC, Cyt *c*, and Hgb and alkylated proteins (2 mg/ml) were incubated with 500 μ M GO or MGO at pH 7.4 for 72 h and then dialyzed against PBS for 16 h at 4 °C. The samples were then used for LC–MS/MS analysis of CML and CEL.

Protein-thiol estimation

Ten micrograms of dialyzed reduced and alkylated proteins were used to estimate thiol content using the Thiol Quantification Assay Kit (Abcam), with reduced GSH as the standard.

TNBS assay

RA or control protein (200 μ g/0.3 ml) was incubated with 0.15 ml of 0.01% TNBS in 0.1M sodium bicarbonate buffer, pH 8.5, at room temperature for 2 h. After incubation, 0.15 ml of 10% SDS was added, and the reaction was neutralized by adding 0.075 ml of 1 M HCl. The absorbance was measured at 335 nm.

CD measurements

Far- and near-UV CD spectra were recorded in a Chirascan Plus spectrometer (Applied Photophysics) at 25 °C. Far-UV CD recorded at spectral wavelength from 260 to 190 nm

with a scanning speed of 50 nm/min and a 1 nm bandwidth. A concentration of 0.25 mg/ml was used for WT- α AC or mutated α AC. The spectra were measured using quartz cuvettes with a path length of 1 mm for far-UV CD.

Fluorescence measurements

Intrinsic fluorescence spectra of WT- α AC or mutant α AC (0.25 mg/ml) were recorded in a spectrofluorometer (Fluoromax 4P; Horiba Jobin Mayer). The excitation wavelength used was 280 nm. The emission spectra were recorded between 310 and 450 nm. The excitation and emission slit widths were 2.5 and 5 nm, respectively.

Hemithioacetal formation and incubation with Boc-Lys

GSH (5 mM) was mixed with GO (5 mM), and the hemithioacetal formation was measured at 290 nm over 100 min. Five micrograms of GLO1 was added to a 50 min preincubated GO + GSH mixture, and the hemithioacetal decrease was monitored. In some samples, Boc-Lys (5 mM) was added to a 50 min preincubated GO + GSH mixture. In other samples, heat-inactivated GLO1 (~65 °C for 3 min) was added to the mixture of GO + GSH + Boc-Lys. The hemithioacetal level was measured at 290 nm at 0, 4, 24, and 48 h. Subsequently, the CML level was measured at 0, 24, and 48 h.

Statistics

The data are presented as the mean \pm SD, based on experiments conducted with at least three samples. Two groups were compared using an unpaired Student's *t* test, whereas multiple groups were compared using one-way ANOVA multiple comparison tests.

Data availability

All data are contained within the article.

Supporting information—This article contains supporting information (37).

Acknowledgments—We thank Dr Mi-Hyun Nam for the valuable feedback on the article. This work was supported by the National Institutes of Health grants EY023286 and EY033915 and an unrestricted grant from Research to Prevent Blindness to the Department of Ophthalmology, University of Colorado.

Author contributions—M. A. G. and R. H. N. conceptualization; S. P. and C. M. validation; S. P., J. R., C. M., M. A. G., and R. H. N. formal analysis; S. P., J. R., C. M., and G. C. investigation; S. P., J. R., C. M., and G. C. data curation; S. P., J. R., C. M., M. A. G., and R. H. N. writing—original draft; S. P., J. R., C. M., M. A. G., and R. H. N. writing—review & editing; R. H. N. supervision; R. H. N. funding acquisition.

Funding and additional information—The mass spectrometry facility at the Skaggs School of Pharmacy and Pharmaceutical Sciences, University of Colorado, Anschutz Medical Campus is supported by the National Institutes of Health-National Center for Research Resources grant 1S10OD028538-01A1 (to N.A.

Reisdorph). The content is solely the responsibility of the authors and does not necessarily represent the official views of the National Institutes of Health.

Conflict of interest—The authors declare that they have no conflicts of interest with the contents of the article.

Abbreviations—The abbreviations used are: AcCoA, acetyl CoA; AcK, acetylation of lysine; AGE, advanced glycation end product; α AC, α A-crystallin; α BC, α B-crystallin; Boc-Lys, t-Boc-lysine; CEL, N^ε-carboxyethyllysine; CML, N^ε-carboxymethyllysine; Cyt c, cytochrome c; GA, glycolaldehyde; GLO1, glyoxalase I; GO, glyoxal; GOLD, glyoxal lysine-dimer; Hgb, hemoglobin; HSA, human serum albumin; MGO, methylglyoxal; MOLD, methylglyoxal lysine-dimer; NAC, N-acetylcysteine; NEM, N-ethyl maleimide; RA, reductive alkylation; RAGE, receptor for AGE; γ SC, γ S-crystallin; TCEP, Tris(2-carboxyethyl)phosphine hydrochloride; TNBS, 2,4,6-trinitrobenzenesulfonic acid.

References

- Goldin, A., Beckman, J. A., Schmidt, A. M., and Creager, M. A. (2006) Advanced glycation end products - sparking the development of diabetic vascular injury. *Circulation* **114**, 597–605
- Twarda-Clapa, A., Olczak, A., Bialkowska, A. M., and Koziolkiewicz, M. (2022) Advanced glycation end-products (AGEs): formation, chemistry, classification, receptors, and diseases related to AGEs. *Cells* **11**, 1312
- Chaudhuri, J., Bains, Y., Guha, S., Kahn, A., Hall, D., Bose, N., *et al.* (2018) The role of advanced glycation end products in aging and metabolic diseases: bridging association and causality. *Cell Metab.* **28**, 337–352
- Aragno, M., and Mastrocola, R. (2017) Dietary sugars and endogenous formation of advanced glycation endproducts: emerging mechanisms of disease. *Nutrients* **9**, 385
- Ulrich, P., and Cerami, A. (2001) Protein glycation, diabetes, and aging. *Recent Prog. Horm. Res.* **56**, 1–21
- Linetsky, M., Shipova, E., Cheng, R. Z., and Ortwerth, B. J. (2008) Glycation by ascorbic acid oxidation products leads to the aggregation of lens proteins. *BBA-Mol. Basis. Dis.* **1782**, 22–34
- Scheffler, J., Bork, K., Bezold, V., Rosenstock, P., Gnanapragassam, V. S., and Horstkorte, R. (2019) Ascorbic acid leads to glycation and interferes with neurite outgrowth. *Exp. Gerontol.* **117**, 25–30
- Sharma, C., Kaur, A., Thind, S. S., Singh, B., and Raina, S. (2015) Advanced glycation End-products (AGEs): an emerging concern for processed food industries. *J. Food Sci. Tech. Mys.* **52**, 7561–7576
- Vistoli, G., De Maddis, D., Cipak, A., Zarkovic, N., Carini, M., and Aldini, G. (2013) Advanced glycoxidation and lipoxidation end products (AGEs and ALEs): an overview of their mechanisms of formation. *Free Radic. Res* **47**, 3–27
- Berends, E., van Oostenbrugge, R. J., Foulquier, S., and Schalkwijk, C. G. (2023) Methylglyoxal, a highly reactive dicarbonyl compound, as a threat for blood brain barrier integrity. *Fluids Barriers CNS* **20**, 75
- Altomare, A., Baron, G., Gianazza, E., Banfi, C., Carini, M., and Aldini, G. (2021) Lipid peroxidation derived reactive carbonyl species in free and conjugated forms as an index of lipid peroxidation: limits and perspectives. *Redox Biol.* **42**, 101899
- Fuloria, S., Subramaniam, V., Karupiah, S., Kumari, U., Sathasivam, K., Meenakshi, D. U., *et al.* (2020) A comprehensive review on source, types, effects, nanotechnology, detection, and therapeutic management of reactive carbonyl species associated with various chronic diseases. *Antioxidants* **9**, 1075
- McEwen, J. M., Fraser, S., Guir, A. L. S., Dave, J., and Scheck, R. A. (2021) Synergistic sequence contributions bias glycation outcomes. *Nat. Commun.* **12**, 3316
- Lko, A. B. S., Gostomska-Pampuch, K., Kuzan, A., Pietkiewicz, J., Krzystek-Korpacka, M. L., and Gaman, A. (2024) Effect of advanced

Proximal cysteine residues facilitate N^ε-carboxylation

- glycation end-products in a wide range of medical problems including COVID-19. *Adv. Med. Sci-Poland* **69**, 36–50
- Glomb, M. A., and Lang, G. (2001) Isolation and characterization of glyoxal-arginine modifications. *J. Agric. Food Chem.* **49**, 1493–1501
 - Nandi, S. K., Nahomi, R. B., Rankenberg, J., Glomb, M. A., and Nagaraj, R. H. (2020) Glycation-mediated inter-protein cross-linking is promoted by chaperone-client complexes of α -crystallin: implications for lens aging and presbyopia. *J. Biol. Chem.* **295**, 5701–5716
 - Sparvero, L. J., Asafu-Adjei, D., Kang, R., Tang, D. L., Amin, N., Im, J., et al. (2009) RAGE (receptor for advanced glycation endproducts), RAGE ligands, and their role in cancer and inflammation. *J. Transl. Med.* **7**, 17
 - Singh, V. P., Bali, A., Singh, N., and Jaggi, A. S. (2014) Advanced glycation end products and diabetic complications. *Korean J. Physiol. Pha.* **18**, 1–14
 - Rowan, S., Bejarano, E., and Taylor, A. (2018) Mechanistic targeting of advanced glycation end-products in age-related diseases. *BBA-Mol. Basis. Dis.* **1864**, 3631–3643
 - Salazar, J., Navarro, C., Ortega, A., Nava, M., Morillo, D., Torres, W., et al. (2021) Advanced glycation end products: new clinical and molecular perspectives. *Int. J. Env. Res. Pub. He.* **18**, 7236
 - Nascimento, M. M., Suliman, M. E., Murayama, Y., Nih, M., Hayashi, S. Y., Stenvinkel, P., et al. (2006) Effect of high-dose thiamine and pyridoxine on advanced glycation end products and other oxidative stress markers in hemodialysis patients: a randomized placebo-controlled study. *J. Ren. Nutr.* **16**, 119–124
 - Fan, X. J., and Monnier, V. M. (2021) Protein posttranslational modification (PTM) by glycation: role in lens aging and age-related cataractogenesis. *Exp. Eye Res.* **210**, 108705
 - Vazquez, S., Aquilina, J. A., Jamie, J. F., Sheil, M. M., and Truscott, R. J. W. (2002) Novel protein modification by kynurenine in human lenses. *J. Biol. Chem.* **277**, 4867–4873
 - Sharma, K. K., and Santhoshkumar, P. (2009) Lens aging: effects of crystallins. *Biochim. Biophys. Acta* **1790**, 1095–1108
 - Fan, X. J., Monnier, V. M., and Whitson, J. (2017) Lens glutathione homeostasis: discrepancies and gaps in knowledge standing in the way of novel therapeutic approaches. *Exp. Eye Res.* **156**, 103–111
 - Ortwerth, B. J., and Olesen, P. R. (1988) Glutathione inhibits the glycation and crosslinking of lens proteins by ascorbic-acid. *Exp. Eye Res.* **47**, 737–750
 - Kisic, B., Miric, D., Zoric, L., Ilic, A., and Dragojevic, I. (2012) Antioxidant capacity of lenses with age-related cataract. *Oxid. Med. Cell Longev.* **2012**, 467130
 - Nagaraj, R. H., Linetsky, M., and Stitt, A. W. (2012) The pathogenic role of Maillard reaction in the aging eye. *Amino Acids* **42**, 1205–1220
 - Franke, S., Dawczynski, J., Strobel, J., Niwa, T., Stahl, P., and Stein, G. (2003) Increased levels of advanced glycation end products in human cataractous lenses. *J. Cataract Refr. Surg.* **29**, 998–1004
 - Nandi, S. K., Rankenberg, J., Rakete, S., Nahomi, R. B., Glomb, M. A., Linetsky, M. D., et al. (2021) Glycation-mediated protein crosslinking and stiffening in mouse lenses are inhibited by carboxitin. *Glycoconjugate J.* **38**, 347–359
 - Slight, S. H., Prabhakaram, M., Shin, D. B., Feather, M. S., and Ortwerth, B. J. (1992) The extent of N-Epsilon-(Carboxymethyl)Lysine formation in lens proteins and polylysine by the autoxidation products of ascorbic-acid. *Biochim. Biophys. Acta* **1117**, 199–206
 - Glomb, M. A., and Monnier, V. M. (1995) Mechanism of protein modification by glyoxal and glycolaldehyde, reactive intermediates of the maillard reaction. *J. Biol. Chem.* **270**, 10017–10026
 - Lyons, T. J., Silvestri, G., Dunn, J. A., Dyer, D. G., and Baynes, J. W. (1991) Role of glycation in modification of lens crystallins in diabetic and nondiabetic senile cataracts. *Diabetes* **40**, 1010–1015
 - Schwarzenbolz, U., and Henle, T. (2009) Cysteine mediated formation of ϵ -Carboxymethyllysine (CML) on proteins. *Czech J. Food Sci.* **27**, S156–S159
 - Schwarzenbolz, U., Mende, S., and Henle, T. (2008) Model studies on protein glycation - influence of cysteine on the reactivity of arginine and lysine residues toward glyoxal. *Ann. Ny. Acad. Sci.* **1126**, 248–252
 - Panja, S., Nahomi, R. B., Rankenberg, J., Michel, C. R., and Nagaraj, R. H. (2024) Thiol-mediated enhancement of N^ε-acetyllysine formation in lens proteins. *ACS Chem. Biol.* **19**, 1495–1505
 - Di Sanzo, S., Spengler, K., Leheis, A., Kirkpatrick, J. M., Randler, T. L., Baldensperger, T., et al. (2021) Mapping protein carboxymethylation sites provides insights into their role in proteostasis and cell proliferation. *Nat. Commun.* **12**, 6743
 - Gaffney, D. O., Jennings, E. Q., Anderson, C. C., Marentette, J. O., Shi, T., Oxvig, A. M. S., et al. (2020) Non-enzymatic lysine lactoylation of glycolytic enzymes. *Cell Chem. Biol.* **27**, 206–213
 - Glomb, M. A., and Pfahler, C. (2001) Amides are novel protein modifications formed by physiological sugars. *J. Biol. Chem.* **276**, 41638–41647
 - Eggen, M. D., and Glomb, M. A. (2021) Novel amidine protein cross-links formed by the reaction of glyoxal with lysine. *J. Agric. Food Chem.* **69**, 7960–7968
 - Coukos, J. S., and Moellering, R. E. (2021) Methylglyoxal forms diverse mercaptomethylimidazole crosslinks with thiol and guanidine pairs in endogenous metabolites and proteins. *ACS Chem. Biol.* **16**, 2453–2461
 - Kislinger, T., Fu, C., Huber, B., Qu, W., Taguchi, A., Du Yan, S., et al. (1999) N^ε-(Carboxymethyl)Lysine adducts of proteins are ligands for receptor for advanced glycation end products that activate cell signaling pathways and modulate gene expression. *J. Biol. Chem.* **274**, 31740–31749
 - Xue, J., Rai, V., Singer, D., Chabierski, S., Xie, J., Reverdatto, S., et al. (2011) Advanced glycation end product recognition by the receptor for AGEs. *Structure* **19**, 722–732
 - Ramasamy, R., Vannucci, S. J., Yan, S. S., Herold, K., Yan, S. F., and Schmidt, A. M. (2005) Advanced glycation end products and RAGE: a common thread in aging, diabetes, neurodegeneration, and inflammation. *Glycobiology* **15**, 16R–28R
 - Egana-Gorrone, L., Lopez-Diez, R., Yepuri, G., Ramirez, L. S., Reverdatto, S., Gugger, P. F., et al. (2020) Receptor for advanced glycation end products (RAGE) and mechanisms and therapeutic opportunities in diabetes and cardiovascular disease: insights from human subjects and animal models. *Front. Cardiovasc. Med.* **7**, 37
 - Song, Q. H., Liu, J. J., Dong, L. Y., Wang, X. L., and Zhang, X. D. (2021) Novel advances in inhibiting advanced glycation end product formation using natural compounds. *Biomed. Pharmacother.* **140**, 111750
 - Rabbani, N., and Thornalley, P. J. (2022) Emerging glycation-based therapeutics-glyoxalase 1 inducers and glyoxalase 1 inhibitors. *Int. J. Mol. Sci.* **23**, 2453
 - Nagaraj, R. H., Nahomi, R. B., Shanthakumar, S., Linetsky, M., Padmanabha, S., Pasupuleti, N., et al. (2012) Acetylation of alphaA-crystallin in the human lens: effects on structure and chaperone function. *Biochim. Biophys. Acta* **1822**, 120–129
 - Panja, S., Nahomi, R. B., Rankenberg, J., Michel, C. R., Gaikwad, H., Nam, M. H., et al. (2023) Aggrelyte-2 promotes protein solubility and decreases lens stiffness through lysine acetylation and disulfide reduction: implications for treating presbyopia. *Aging Cell* **22**, e13797
 - Panja, S., Nam, M. H., Gaikwad, H., Rankenberg, J., and Nagaraj, R. H. (2023) Topical ocular application of aggrelyte-2A reduces lens stiffness in mice. *Front. Ophthalmol.* **3**, 1274825
 - Panja, S., Gaikwad, H., Rankenberg, J., Nam, M. H., and Nagaraj, R. H. (2023) Promotion of protein solubility and reduction in stiffness in human lenses by aggrelyte-1: implications for reversing presbyopia. *Int. J. Mol. Sci.* **24**, 2196
 - Korwar, A. M., and Zhang, Q. (2021) Comprehensive quantification of carboxymethyllysine-modified peptides in human plasma. *J. Am. Soc. Mass Spectrom.* **32**, 744–752
 - Kumari, N., Bandyopadhyay, D., Kumar, V., Venkatesh, D. B., Prasad, S., Prakash, S., et al. (2021) Glycation of albumin and its implication in Diabetes: a comprehensive analysis using mass spectrometry. *Clin. Chim. Acta* **520**, 108–117
 - Dunn, J. A., Patrick, J. S., Thorpe, S. R., and Baynes, J. W. (1989) Oxidation of glycated proteins - age-dependent accumulation of N-Epsilon-(Carboxymethyl)Lysine in lens proteins. *Biochemistry* **28**, 9464–9468
 - Giblin, F. J. (2000) Glutathione: a vital lens antioxidant. *J. Ocul. Pharmacol. Th.* **16**, 121–135

56. Liu, R. B., Yue, Z., Tsai, C. C., and Shen, J. N. (2019) Assessing lysine and cysteine reactivities for designing targeted covalent kinase inhibitors. *J. Am. Chem. Soc.* **141**, 6553–6560
57. Andreeva, A., Bekkhozhin, Z., Omertassova, N., Baizhumanov, T., Yeltay, G., Akhmetali, M., *et al.* (2019) The apparent deglycase activity of DJ-1 results from the conversion of free methylglyoxal present in fast equilibrium with hemithioacetals and hemiaminals. *J. Biol. Chem.* **294**, 18863–18872
58. Wensien, M., von Pappenheim, F. R., Funk, L. M., Kloskowski, P., Curth, U., Diederichsen, U., *et al.* (2021) A lysine-cysteine redox switch with an NOS bridge regulates enzyme function. *Nature* **593**, 460–464
59. Rankenberg, J., Rakete, S., Wagner, B. D., Patnaik, J. L., Henning, C., Lynch, A., *et al.* (2021) Advanced glycation end products in human diabetic lens capsules. *Exp. Eye Res.* **210**, 108704